JACS
JOURNAL OF THE AMERICAN CHEMICAL SOCIETY

Article

pubs.acs.org/JACS

Ultrafast Vibrational Dynamics and Energy Transfer in Imidazolium Ionic Liquids

Mahesh Namboodiri,[†] Mehdi Mohammad Kazemi,[†] Tahir Zeb Khan,[†] Arnulf Materny,*[,†] and Johannes Kiefer*[,‡,§]

[†]Center for Functional Materials and Nanomolecular Science, Jacobs University, Campus Ring 1, D-28759 Bremen, Germany

[‡]School of Engineering, Fraser Noble Building, University of Aberdeen, Aberdeen AB24 3UE, U.K.

[§]Technische Thermodynamik, Universität Bremen, Badgasteiner Straße 1, D-28359 Bremen, Germany

Supporting Information

ABSTRACT: Femtosecond time-resolved coherent anti-Stokes Raman scattering (CARS) is used as a probe for monitoring the vibrational dynamics of room temperature ionic liquids (ILs). The experiments are performed on a series of 1,3-dialkylimidazolium ILs containing the bis-(trifluoromethylsulfonyl)imide [NTf_2] anion. The effect of methylation of the cationic C2 position on the dephasing time is studied analyzing [NTf_2]-ILs of 1-ethyl-3-methylimidazolium [EMIM], 1-ethyl-2,3-dimethylimidazolium [EMMIM], 1-butyl-3-methylimidazolium [BMIM], and 1-butyl-2,3-dimethylimidazolium [BMMIM]. Raman coherences are excited around ~1400 cm^{-1}, and the vibrational dephasing of the modes in the fingerprint region is monitored as a function of time. The results indicate that vibrational energy transfer occurs governed by the interionic interactions. This is suggested by mode beating involving vibrations beyond the excitation spectrum as well as systematic differences in the temporal dephasing behavior. In contrast, the length of the cationic alkyl side chain has a negligible impact on the vibrational dynamics.

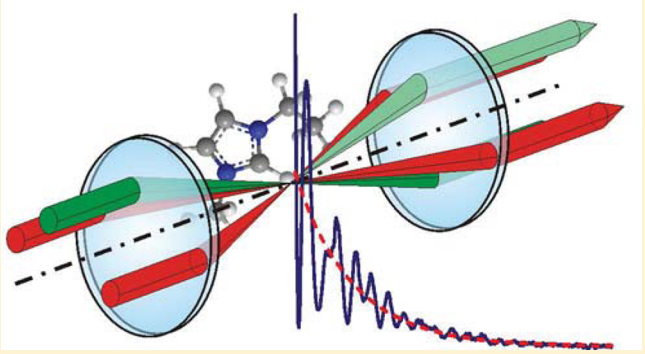

INTRODUCTION

Unique properties including high electro-conductivity and negligible vapor pressure make many room-temperature ionic liquids (ILs) interesting alternative fluids for use in practical applications in areas as diverse as electrochemistry, separation technology, and catalysis.[1−6] The macroscopic properties of an IL are determined by its molecular structure and by the interactions between the ions. The latter may include classical ionic and polar interactions but also hydrogen bonding and dispersive forces.[7−9] Consequently, in order to allow an IL with optimal properties for a specific application to be designed, the structure and interactions, as well as their effects must be fully understood.[10−12] For this purpose, spectroscopic methods have been proved very useful. In particular, vibrational spectroscopic techniques such as Raman and IR spectroscopy are frequently employed for providing information about structure and interactions in the frequency domain. However, the Raman and IR data do not provide insights into the vibrational dynamics, which occur at ultrafast time scales in the order of femto- and picoseconds. Only a few studies using ultrafast time-resolved spectroscopic methods for analyzing ILs have been reported though. Iwata et al.[13] employed a picosecond coherent anti-Stokes Raman scattering (CARS) setup to probe the local structure formation of imidazolium based ionic liquids. Giraud et al.[14] used heterodyne-detected Raman-induced Kerr effect spectroscopy to study the effect of anion and cation substitution on the ultrafast dynamics of room temperature ionic liquids. Turton et al.[15] used optical Kerr effect spectroscopy for the relaxation behavior of aggregates and clusters forming in ILs.

Femtosecond CARS is a suitable technique to study ultrafast vibrational dynamics in the time domain. In CARS, two laser pulses (called the pump and Stokes pulses), the frequency difference of which matches one or more Raman transitions of the molecule of interest, create a Raman coherence. A third probe pulse interacts with this coherent state to create the anti-Stokes signal. In fs-CARS, the probe pulse is delayed in time with respect to the pump and Stokes pulses, and by systematically varying this delay the ultrafast dynamics of the molecular vibrations can be monitored.[16−18] We note that in principle the decay rates of vibrational modes can be determined from the line-widths in an isotropic spontaneous Raman spectrum.[19] However, even for very simple gas-phase molecules it was shown recently that time-domain CARS provides a better accuracy in determining decay times than high-resolution frequency-domain measurements.[20]

Received: March 12, 2014
Published: April 3, 2014

dx.doi.org/10.1021/ja502527y | J. Am. Chem. Soc. 2014, 136, 6136−6141

In this work, we present the first study of vibrational dynamics in a series of ionic liquids with sytematically varied ions using femtosecond time-resolved CARS. Note that fs-CARS has been applied to ILs recently by another group,[21] but the fixed time delay did not allow the transients to be studied. The effects of methylation of the C2 position of 1,3-dialkylimidazolium-based ILs on the dephasing time is monitored by analyzing a set of ILs containing the bis-(trifluoromethylsulfonyl)imide [NTf_2] anion and the cations 1-ethyl-3-methylimidazolium [EMIM], 1-ethyl-2,3-dimethylimidazolium [EMMIM], 1-butyl-3-methylimidazolium [BMIM] and 1-butyl-2,3-dimethylimidazolium [BMMIM]. The stucture of these ions is shown schematically in Figure 1. The

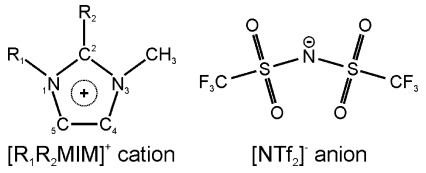

Figure 1. Structure of the imidazolium cation and NTf_2 anion. The moieties R_1 and R_2 represent ethyl or butyl chains and hydrogen or methyl, repectively.

compounds have been selected as their vibrational spectra as well as the structure–property relationships are well understood. The results are discussed against those from frequency domain spectroscopy published in previous papers.[22−25]

EXPERIMENTAL SECTION

The experimental setup is shown in Figure 2. The 150 fs (775 nm, 1 kHz repetition rate, 1 mJ energy/pulse) pulses from the regeneratively

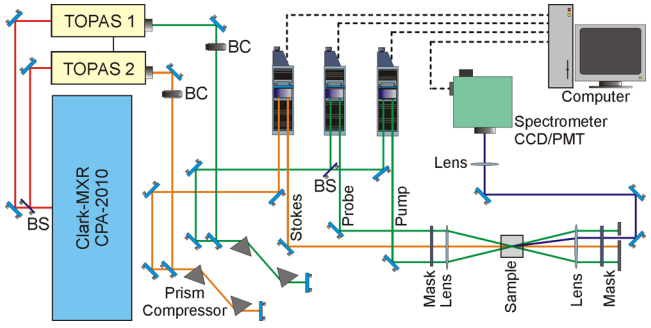

Figure 2. Sketch of the experimental setup used for the femtosecond time-resolved CARS experiments (BS = beam splitter, BC = Berek compensator for polarization rotation).

amplified Ti:sapphire laser (CPA 2010, Clark MXR) are used to pump two optical parametric amplifiers (TOPAS, Light Conversion). The pulses are compressed to ~80 fs using prism pair set-ups. The output of the first OPA is split into two equal parts to obtain independent pump and probe pulses used in the degenerate pump–probe CARS experiment. The other OPA serves as source for the Stokes pulse. The timing of the individual pulses was controlled by using computer-controlled delay stages in a Michelson interferometer-like setup. Moreover, the pulses were aligned into a three-dimensional folded BoxCARS arrangement, which fulfils the phase matching condition and allows filtering the anti-Stokes signal spatially. Using a 100 mm lens the pulses were subsequently focused into the sample cell. By monitoring the cross correlation and autocorrelation signals produced in a BBO crystal, the temporal overlap between the three pulses was determined. The CARS signal was collimated and monitored by a monochromator (Triax 180/190, Horiba Jobin Yvon; 1200 lines/mm grating), which helped to filter out background radiation and to disperse the spectrally broad anti-Stokes signal. For detection a CCD detector was used. The signal was recorded as a function of the time delay between the time coincident pump/Stokes pair and the probe pulse. The IL samples were contained in a 2 mm thick cuvette. The total energy at the sample was 10 nJ/pulse. No degradation of the sample was observed during the course of the experiment. This was verified by monitoring the variation in CARS signal intensity over a longer period. The preparation of the ILs is described in detail in previous work.[24]

RESULTS AND DISCUSSION

The frequency difference between the pump (635 nm) and the Stokes (697 nm) beams is tuned to be in resonance with Raman modes of the ILs centered around ~1400 cm^{-1}. This spectral region is dominated by the vibrations of the cation and in particular modes of the imidazolium ring and the butyl side chains in the cases of [BMIM] and [BMMIM]. The ground-state wavepacket evolution is probed by delaying the probe pulse after interaction of the time coincident pump/Stokes pair. The spectral assignments of the vibrational modes mentioned in the following can be found together with a more detailed discussion of the vibrational structures in previous work.[22−25]

Transients. As a first step, the CARS transients highlighting the ultrafast vibrational dynamics will be discussed. Figures 3−6 display the data obtained for [EMIM][NTf_2], [EMMIM]-[NTf_2], [BMIM][NTf_2], and [BMMIM][NTf_2], respectively.

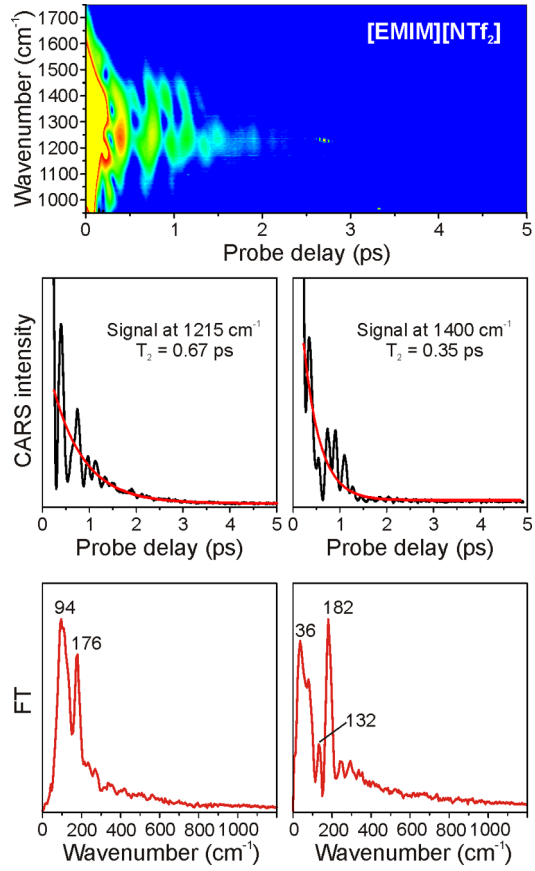

Figure 3. Signals recorded in [EMIM][NTf_2]. The upper contour plot displays the transients as a function of detection wavenumber. The dominating transients at 1215 and 1400 cm^{-1} and their corresponding Fourier transform spectra are plotted below. The red lines in the transient diagrams represent fitted single-exponential functions.

dx.doi.org/10.1021/ja502527y | J. Am. Chem. Soc. 2014, 136, 6136−6141

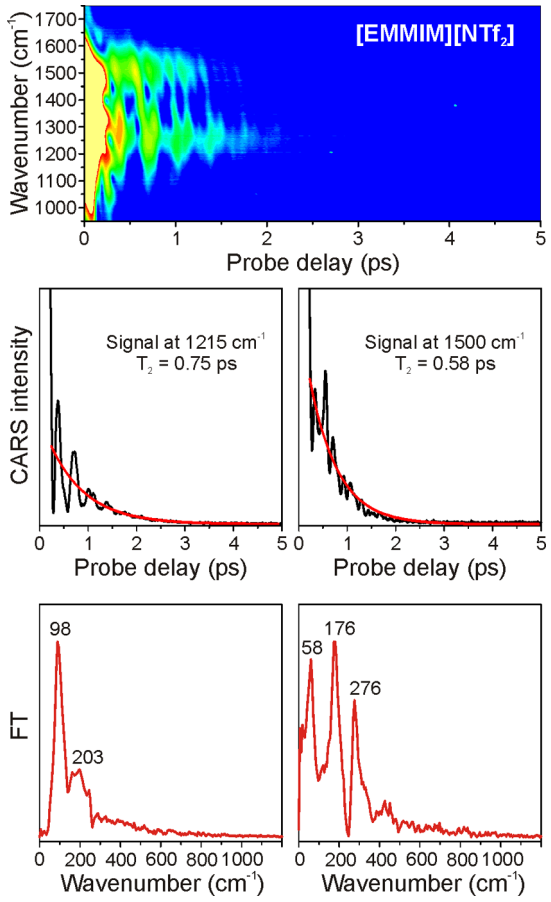

Figure 4. Signals recorded in [EMMIM][NTf_2]. The upper contour plot displays the transients as a function of detection wavenumber. The dominating transients at 1215 and 1500 cm^{-1} and their corresponding Fourier transform spectra are plotted below. The red lines in the transient diagrams represent fitted single-exponential functions.

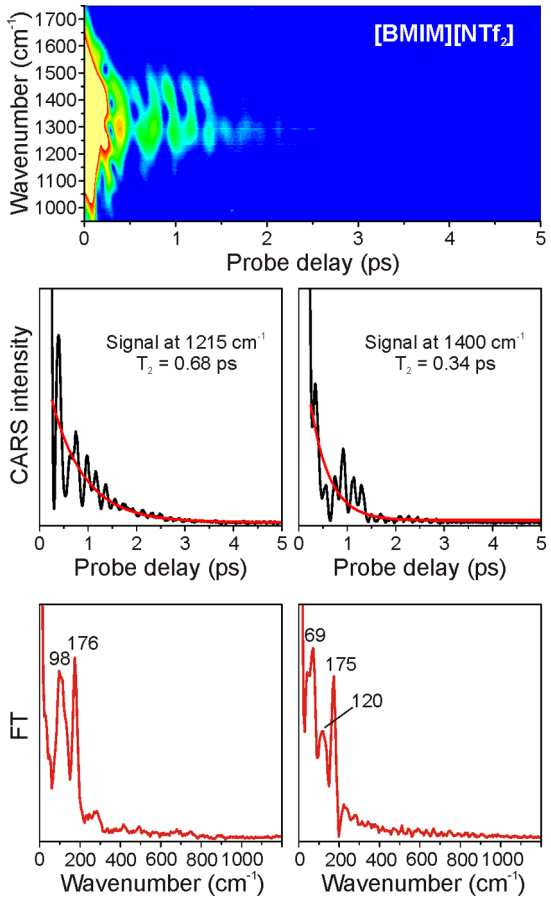

Figure 5. Signals recorded in [BMIM][NTf_2]. The upper contour plot displays the transients as a function of detection wavenumber. The dominating transients at 1215 and 1400 cm^{-1} and their corresponding Fourier transform spectra are plotted below. The red lines in the transient diagrams represent fitted single-exponential functions.

The upper part illustrates a two-dimensional plot of the time-resolved dynamics as a function of the detection wavelength. The contour plots clearly show the dephasing of two modes centered around 1215 and 1400 cm^{-1} for the protonated ILs, and around 1215 and 1500 cm^{-1} for the methylated ILs. CARS transients at the two detection frequencies are given in the diagrams below the 2D plots. In all cases, at $\Delta t = 0$, a sharp peak is observed due to the coherent interaction of all three pulses, which is called the, "coherent artifact". This is due to non-resonant contributions to the CARS polarization possessing very short life times and therefore reflecting the cross correlation of the involved pulses.[16,26] After this strong initial peak of overlapping resonant and non-resonant contributions, the oscillating CARS signal originating from the Raman excitation can be observed. These dynamics show a complex temporal behavior and decay within about 2 ps. In fact, the signals represent the superimposed beating between pairs of vibrational modes. In order to extract more quantitative information the transients were fitted with an exponential function providing the dephasing time T_2. A fit including all beating dynamics would have yielded more detailed information. However, the considerable number of fitting parameters did not result in an unambiguous data set for the relatively short transients. Therefore, only the average dephasing time T_2 could be obtained (compare, e.g. ref 27). In addition, the Fourier transform (FT) spectra of the transients were computed and reveal the vibrational as well as rotational energy spacings seen as mode beatings. The peaks in the FT represent coherences between nearest neighbor vibrational modes.

For [EMIM][NTf_2], the major peaks in the FT spectra for 1215 cm^{-1} are 94 and 176 cm^{-1}, which correspond to the beating between vibrational modes at 1319/1225 (94) and 1118/942 (176) cm^{-1}. With the exception of the imidazolium ring mode at 942 cm^{-1}, the modes involved in the beating can all be assigned to vibrations of the [NTf_2] anion: those at 1319 and 1225 cm^{-1}, to the asymmetric stretch, and the 1118 cm^{-1}, to the symmetric stretch of SO_2 (for completeness, the mode 1319 cm^{-1} contains contributions from ring vibration in the cation). The peaks in the FT spectrum of the transient detected at 1400 cm^{-1} can be assigned to the beating between modes at 1444/1407 (36), 1407/1319 (78), 1444/1319 (132), and 1407/1225 (182) cm^{-1}. The signals at 1444 and 1407 cm^{-1} correspond to symmetric bending and asymmetric stretching modes of the imidazolium ring. The dephasing time T_2 is almost a factor of 2 longer for 1215 cm^{-1} (0.67 ps) than for 1400 cm^{-1} (0.35 ps).

The contour plot of [EMMIM][NTf_2] shown in Figure 4 reveals the dephasing of two modes centered around 1215 and 1500 cm^{-1}. The major peaks in the FT spectra for 1215 cm^{-1} are 98 and 203 cm^{-1}, which correspond to the beating between

dx.doi.org/10.1021/ja502527y | J. Am. Chem. Soc. 2014, 136, 6136−6141

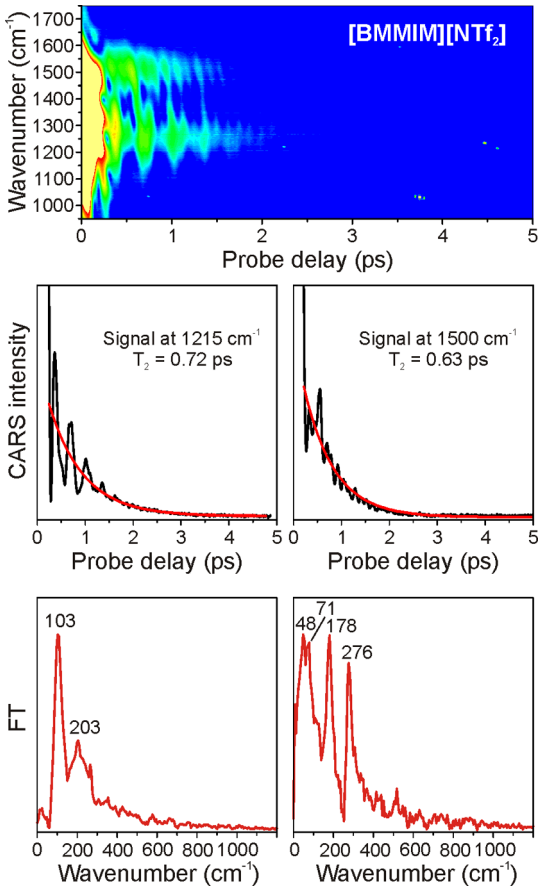

Figure 6. Signals recorded in [BMMIM][NTf_2]. The upper contour plot displays the transients as a function of detection wavenumber. The dominating transients at 1215 and 1500 cm^{-1} and their corresponding Fourier transform spectra are plotted below. The red lines in the transient diagrams represent fitted single-exponential functions.

vibrational modes at 1323/1225 (98) and 1323/1120 (203) cm^{-1}. The 1323 cm^{-1} mode can be assigned to the asymmetric stretch of the anionic SO_2 and cationic ring vibrations, the 1225 and 1120 cm^{-1} ones to the asymmetric stretch and the symmetric stretches of SO_2, respectively. The FT peaks at 1500 cm^{-1} can be assigned to the beating between modes at 1499/1444 (58), 1499/1323 (176), and 1499/1225 (276) cm^{-1}. The 1499 and 1444 cm^{-1} signals correspond to an $NC(CH_3)N$ CC stretch, respectively, a band with overlapping contributions of different imidazolium ring vibrations. The dephasing time T_2 shows a less significant difference than in [EMIM][NTf_2]; 0.75 ps at 1215 cm^{-1} and 0.58 ps at 1500 cm^{-1}.

The data obtained for [BMIM][NTf_2] showing major peaks in the FT spectra for 1215 cm^{-1} are 98 and 176 cm^{-1}, which correspond to the beating between vibrational modes at 1321/1223 (98) and 1223/1046 (176) cm^{-1}. The 1321 cm^{-1} mode can be assigned to the asymmetric stretch of the anionic SO_2 and cationic ring vibrations, the 1223 cm^{-1} one to the asymmetric SO_2 stretch. The 1046 cm^{-1} mode is predominantly due to CC stretching in the butyl side chain. The FT peaks at 1400 cm^{-1} can be assigned to the beating between modes at 1442/1373 (69), 1442/1321 (120), and 1405/1223 (176) cm^{-1}. The signals at 1442 and 1405 cm^{-1} correspond to symmetric bending and asymmetric stretching modes of the imidazolium ring. The signal at 1373 cm^{-1} belongs to ring vibrations. In the case of [BMIM][NTf_2], the dephasing time T_2 is again a factor of 2 longer for 1215 cm^{-1} (0.68 ps) than 1400 cm^{-1} (0.34 ps).

For the IL [BMMIM][NTf_2], the major peaks in the FT spectra for 1215 cm^{-1} are 98 and 203 cm^{-1}, which correspond to the beating between vibrational modes at 1223/1120 (103) and 1323/1120 (203) cm^{-1}. The 1323 cm^{-1} mode can be assigned to the asymmetric stretch the anionic SO_2 and cationic ring vibrations, the 1223 and 1120 cm^{-1} ones to the asymmetric stretch and the symmetric stretches of SO_2, respectively. The FT peaks at 1500 cm^{-1} can be assigned to the beating between modes at 1371/1323 (48), 1442/1371 (71), 1499/1323 (178), and 1499/1223 (276) cm^{-1}. The 1499 and 1442 cm^{-1} signals correspond to an $NC(CH_3)N$ CC stretch, respectively, a band with overlapping contributions of different imidazolium ring vibrations. The 1371 cm^{-1} mode belongs to vibrations of the imidazolium ring. The dephasing time T_2 is determined to be 0.72 ps at 1215 cm^{-1} and 0.63 ps at 1500 cm^{-1}.

Vibrational Energy Transfer. The above findings have implications for the ultrafast physicochemical behavior of the ILs under investigation. In [EMIM][NTf_2], it is interesting that the mode at 942 cm^{-1} is involved in the beating. The laser bandwidth is in the order of 180−190 cm^{-1}, and hence the bandwidth of the pump and Stokes pulses only allows the direct excitation of the 1319, 1225, and 1118 cm^{-1} Raman modes. Consequently, the appearance of CARS signals involving the 942 cm^{-1} vibration indicates an ultrafast vibrational energy transfer, which has not been reported in the literature to the best of our knowledge. A similar conclusion can be drawn for the 1046 cm^{-1} mode of [BMIM][NTf_2].

A critical point in drawing the conclusion that the observations are due to vibrational energy transfer is to exclude the possibility of direct excitation by the wings of the laser spectrum. There are a number of arguments why the observed signals do originate from energy transfer and not from laser wing excitation. (1) In general, it must be stressed that CARS is a nonlinear optical process, which means that Raman modes located in the center of the excitation profile are strongly enhanced, while the Raman modes on the wings get very weak or are even completely suppressed relative to the center ones. In the Supporting Information (SI) the excitation profile of the pump and Stokes pulses is plotted together with the Raman spectrum of [EMIM][NTf_2] in Figure S1 of the SI. The mode at 942 cm^{-1} would not be sufficiently excited even if the intensity in the laser wings was increased significantly. (2) Further evidence that those modes were not excited by the wing of the laser spectrum was provided by the CARS transients recorded in other imidazolium ionic liquids. The example of [EMIM] ethylsulfate is presented in Figure S1 of the SI, revealing that such laser wing excitation can be excluded. A detailed vibrational spectroscopic investigation of [EMIM] ethylsulfate can be found in the literature.[22,23] The Raman modes of [EMIM] ethylsulfate around 900−1000 cm^{-1} are strong (compared to those of [EMIM][NTf_2], see Figure S1 of the SI), and hence, they would definitely be excited by the laser wing (if that was the case for [EMIM][NTf_2]), but the experimental signal does not contain beatings involving these modes. (3) In another set of experiments, the excitation profile was shifted to be centered at around 1060 cm^{-1}. If the laser wings would result in an excitation of CARS signals, the two-dimensional contour plots would show a dynamic structure at 1400 cm^{-1} for [EMIM][NTf_2] (which is shown as an example

dx.doi.org/10.1021/ja502527y | J. Am. Chem. Soc. 2014, 136, 6136−6141

in Figure S3 of the SI). However, they do not for any of the ionic liquids studied herein. (4) Furthermore, the transients after 1060 cm^{-1} excitation do not exhibit dephasing rates as short as the ones that can be observed when the proposed vibrational energy transfer after 1400 cm^{-1} excitation takes place. This difference in decay rates provides further strong support that the underlying molecular physics are different. In conclusion, the excitation of the 942 cm^{-1} mode by the laser wings can be excluded in the 1400 cm^{-1} case, and consequently, the observed effect can be clearly assigned to a vibrational energy transfer.

In the methylated [EMMIM][NTf_2] and [BMMIM][NTf_2] ILs, such modes relatively far off the excitation range were not observed. This indicates that the interionic interactions play an important role in this vibrational energy transfer. This hypothesis is corroborated by a comparison of the dephasing times. In the two ILs with protonated C2, the dephasing time of the 1215 cm^{-1} transient is twice the corresponding value at higher frequency, while the methylated ILs do not show such significant differences. The excitation of Raman modes is made predominantly around 1400 cm^{-1}. The modes directly excited seem to partly transfer their energy to modes at lower frequency, hence prolonging the lifetime of the receiving modes and in turn reducing the lifetime of the donating ones as can be seen from the faster decay of the transients. Energy transfer involving hydrogen bonding has been studied to some extent in electronically excited states of dye−solvent complexes; see for instance the work of Zhao and Han[28] and the references therein. They report that hydrogen bonds may be significantly altered (strengthened or weakend) in an excited state and may have an important role in intermolecular charge and energy transfer. However, a direct comparison of these effects with the results of our study is of limited explanatory power as the ILs studied herein are in the electronic ground state.

The effects of the interionic interactions in the ILs studied herein on the vibrational spectra and macroscopic properties have been discussed by Noack et al.[24] against the theories of Fumino et al.[29,30] and Hunt et al.[31,32] It was found that the methylation at the C2 position causes an altered electron density distribution and, as a consequence, changes the position and strength of the interionic interactions. The result is a more stable and regularly packed molecular network with increased Coulombic and decreased van der Waals interactions. In other words, the methylation of the C2 position eliminates the strongly directed and localized hydrogen bonds at the C2 position which leads to higher viscosity and increased melting point. Those conclusions were drawn from peak shifts in Raman-, IR-, and NMR spectra.[24] The present results reveal that the interionic interactions effect not only the vibrational frequencies but also their dynamics. The directional, and compared to other interactions, strong hydrogen bonds in [EMIM][NTf_2] and [BMIM][NTf_2] open a possibility for vibrational energy transfer between the counterions, but they also act as molecular dampers leading to a faster decay in the vibrational dynamics. These observations are consistent for both IL pairs investigated. By contrast, the length of the alkyl side chain is found to have a minor impact on the vibrational dynamics.

SUMMARY AND CONCLUSION

In this paper, we have shown the first time-resolved transients from femtosecond coherent anti-Stokes Raman scattering experiments in imidazolium room-temperature ionic liquids. A systematic variation of cations allowed the influence of the interionic interactions and the alkyl side chain on the vibrational dynamics to be investigated. A key observation was the appearance of mode beatings involving vibrations that were not initially excited by the laser pulses. This indicates a vibrational energy transfer between the ions facilitated by directional hydrogen-bonding interactions. Aside from enabling the energy to be transferred between counterions, the hydrogen bonds act as molecular dampers leading to faster decay of the vibrational dynamics. Our results reveal that conventional frequency domain spectroscopy alone is not sufficient for gaining a detailed understanding of the complex molecular behavior of ionic liquids. Combining frequency and time domain techniques seems to be a promising approach for obtaining a comprehensive picture of the structure−property relationships. This will form the basis for a task-specific development of ILs and consequently make them true designer solvents.

ASSOCIATED CONTENT

Supporting Information

Raman spectra of [EMIM][NTf_2] and [EMIM] ethylsulfate, fs-CARS signals recorded in [EMIM] ethylsulfate with excitation centered at 1400 cm^{-1}, fs-CARS signals recorded in [EMIM]-[NTf_2] with excitation centered at 1060 cm^{-1}. This material is available free of charge via the Internet at http://pubs.acs.org.

AUTHOR INFORMATION

Corresponding Authors

jkiefer@uni-bremen.de (J.K.)
a.materny@jacobs-university.de (A.M.)

Notes

The authors declare no competing financial interest.

ACKNOWLEDGMENTS

Part of this work has been supported by the British Council. J.K. acknowledges membership of the Erlangen Graduate School of Advanced Optical Technologies (SAOT). The Jacobs University group are grateful to Bernd von der Kammer and Dr. Torsten Balster for their continuous support.

REFERENCES

(1) Plechkova, N. V.; Seddon, K. R. *Chem. Soc. Rev.* **2008**, *37*, 123−150.
(2) Welton, T. *Coord. Chem. Rev.* **2004**, *248*, 2459−2477.
(3) Wasserscheid, P.; Keim, W. *Angew. Chem., Int. Ed.* **2000**, *39*, 3773−3789.
(4) Han, X.; Armstrong, D. W. *Acc. Chem. Res.* **2007**, *40*, 1079−1086.
(5) Armand, M.; Endres, F.; MacFarlane, D. R.; Ohno, H.; Scrosati, B. *Nat. Mater.* **2009**, *8*, 621−629.
(6) Galinski, M.; Lewandowski, A.; Stepniak, I. *Electrochim. Acta* **2006**, *51*, 5567−5580.
(7) Kempter, V.; Kirchner, B. *J. Mol. Struct.* **2010**, *972*, 22−34.
(8) Fumino, K.; Wittler, K.; Ludwig, R. *J. Phys. Chem. B* **2012**, *116*, 9507−9511.
(9) Malberg, F.; Pensado, A. S.; Kirchner, B. *Phys. Chem. Chem. Phys.* **2012**, *14*, 12079−12082.
(10) Turner, E. A.; Pye, C. C.; Singer, R. D. *J. Phys. Chem. A* **2003**, *107*, 2277−2288.
(11) Katsyuba, S.; Zvereva, E.; Vidis, A.; Dyson, P. *J. Phys. Chem. A* **2007**, *111*, 352−370.
(12) Slattery, J. M.; Daguenet, C.; Dyson, P. J.; Schubert, T. J. S.; Krossing, I. *Angew. Chem., Int. Ed.* **2007**, *46*, 5384−5388.

(13) Iwata, K.; Okajima, H.; Saha, S.; Hamaguchi, H. *Acc. Chem. Res.* **2007**, *40*, 1174−1181.
(14) Giraud, G.; Gordon, C. M.; Dunkin, I. R.; Wynne, K. *J. Chem. Phys.* **2003**, *119*, 464−477.
(15) Turton, D. A.; Hunger, J.; Stoppa, A.; Hefter, G.; Thoman, A.; Walther, M.; Buchner, R.; Wynne, K. *J. Am. Chem. Soc.* **2009**, *131*, 11140−11146.
(16) Schmitt, M.; Knopp, G.; Materny, A.; Kiefer, W. *J. Phys. Chem. A* **1998**, *102*, 4059−4065.
(17) Namboodiri, M.; Liebers, J.; Kleinekathöfer, U.; Materny, A. *J. Phys. Chem. A* **2012**, *116*, 11341−11346.
(18) Tannor, D. J. *Introduction to Quantum Mechanics: A Time-Dependent Perspective*; University Science Books: Sausalito, 2007.
(19) Loring, R. F.; Mukamel, S. *J. Chem. Phys.* **1985**, *83*, 2116−2128.
(20) Kliewer, C. J.; Gao, Y.; Seeger, T.; Kiefer, J.; Patterson, B. D.; Settersten, T. B. *Proc. Combust. Inst.* **2011**, *33*, 831−838.
(21) Roth, C.; Chatzipapadopoulos, S.; Kerle, D.; Friedriszik, F.; Lutgens, M.; Lochbrunner, S.; Kuhn, O.; Ludwig, R. *New J. Phys.* **2012**, *14*, 105026.
(22) Kiefer, J.; Fries, J.; Leipertz, A. *Appl. Spectrosc.* **2007**, *61*, 1306−1311.
(23) Dhumal, N. R.; Kim, H. J.; Kiefer, J. *J. Phys. Chem. A* **2011**, *115*, 3551−3558.
(24) Noack, K.; Schulz, P. S.; Paape, N.; Kiefer, J.; Wasserscheid, P.; Leipertz, A. *Phys. Chem. Chem. Phys.* **2010**, *12*, 14153−14161.
(25) Dhumal, N. R.; Noack, K.; Kiefer, J.; Kim, H. J. *J. Phys. Chem. A* **2014**, *118*, 2547−2557.
(26) Materny, A.; Chen, T.; Schmitt, M.; Siebert, T.; Vierheilig, A.; Engel, V.; Kiefer, W. *Appl. Phys. B: Laser Opt.* **2000**, *71*, 299−317.
(27) Heid, M.; Chen, T.; Schmitt, M.; Kiefer, W. *Chem. Phys. Lett.* **2001**, *334*, 119−126.
(28) Zhao, G. J.; Han, K. L. *Acc. Chem. Res.* **2012**, *45*, 404−413.
(29) Fumino, K.; Wulf, A.; Ludwig, R. *Angew. Chem., Int. Ed.* **2008**, *47*, 8731−8734.
(30) Fumino, K.; Wulf, A.; Ludwig, R. *Angew. Chem., Int. Ed.* **2008**, *47*, 3830−3834.
(31) Hunt, P. A.; Gould, I. R.; Kirchner, B. *Aust. J. Chem.* **2007**, *60*, 9−14.
(32) Hunt, P. A. *J. Phys. Chem. B* **2007**, *111*, 4844−4853.